Please cite this article in press as: Yang et al., Mechanisms and control of spin interactions in molecular-scale spintronics, Newton (2025), https://doi.org/10.1016/j.newton.2025.100170

Newton

CellPress
OPEN ACCESS

Review

Mechanisms and control of spin interactions in molecular-scale spintronics

Caiyao Yang,[1,3] Hao Wu,[1,3] Jiawen Cao,[1] and Xuefeng Guo[1,2,*]
[1]Beijing National Laboratory for Molecular Sciences, National Biomedical Imaging Center, College of Chemistry and Molecular Engineering, Peking University, 292 Chengfu Road, Haidian District, Beijing 100871, P.R. China
[2]Center of Single-Molecule Sciences, Frontiers Science Center for New Organic Matter, College of Electronic Information and Optical Engineering, Nankai University, 38 Tongyan Road, Jinnan District, Tianjin 300350, P.R. China
[3]These authors contributed equally
*Correspondence: guoxf@pku.edu.cn
https://doi.org/10.1016/j.newton.2025.100170

ACCESSIBLE OVERVIEW Molecular and atomic-scale spintronics lies at the heart of next-generation electronics, where spin-based phenomena promise ultra-fast, low-power devices for potential applications in sensing, data storage, and quantum computing. As researchers delve deeper into spin interactions at these scales, the synergy among spin, electric/magnetic fields, and superconductivity reveals exciting opportunities. This review examines key phenomena such as exchange coupling, the Kondo effect, spin-state transitions, magnetoresistance, and chirality-induced spin selectivity, with a special focus on emerging spin-superconductivity interactions, including Josephson junction effects and Yu-Shiba-Rusinov states. By elucidating these complex interplays, this review aims to shed light on how molecular spin effects can be detected, manipulated, and incorporated into devices, thereby laying essential groundwork for developing robust quantum systems that transcend conventional electronics.

SUMMARY

Molecular-scale spin effects offer potential for nanotechnology and quantum information science, promising ultra-fast, low-power devices and enhanced quantum coherence. However, comprehensive understanding of these phenomena—especially the influence of superconductivity on spin states and coherent spin transport in single-molecule systems—remains limited. This review categorizes spin interactions into three main types, namely spin-spin, spin-field, and spin-superconductivity interactions, examining mechanisms such as exchange coupling, the Kondo effect, field-controlled spin properties, and molecular spin-superconductivity phenomena including single-molecule Josephson junctions. Understanding these interactions is essential for advancing quantum device development.

INTRODUCTION

The utilization of electron spin for information processing dates back to the discovery of the giant magnetoresistance (GMR) effect in 1988,[1,2] a breakthrough that catalyzed the emergence of spintronics and redefined the physical underpinnings of modern information technology. Conventional spintronic devices predominantly rely on bulk magnetic materials or inorganic heterostructures to manipulate spin-polarized currents through external magnetic fields or spin-orbit coupling (SOC). However, as device miniaturization approaches the nanoscale, quantum effects become dominant, necessitating a fundamental shift toward molecular-scale spintronics—a field that focuses on controlling spin states at the level of individual molecules or molecular assemblies to harness quantum effects for advanced functionalities. At this frontier, localized spins in individual molecules or atoms can be precisely engineered, offering unprecedented opportunities for quantum technologies, including spin-based qubits for quantum computing and highly sensitive sensors.[3–5]

The basis of molecular-scale spin control depends on two synergistic pillars: function-driven molecular design and advanced single-molecule manipulation techniques. Chemically tailored spin-active systems—such as organic radicals,[6,7] magnetic metal complexes,[8,9] and chiral molecules[10,11]—serve as ideal candidates for exploring spin-dependent phenomena. For instance, single-molecule magnets (SMMs) stabilize long-lived spin states for quantum information processing,[12–14] while chiral molecules enable spin-selective electron transport.[15,16] Experimentally, techniques like scanning tunneling microscopy (STM), mechanically controllable break junctions (MCBJs), and electromigration-fabricated nanogaps allow the observation

Please cite this article in press as: Yang et al., Mechanisms and control of spin interactions in molecular-scale spintronics, Newton (2025), https://doi.org/10.1016/j.newton.2025.100170

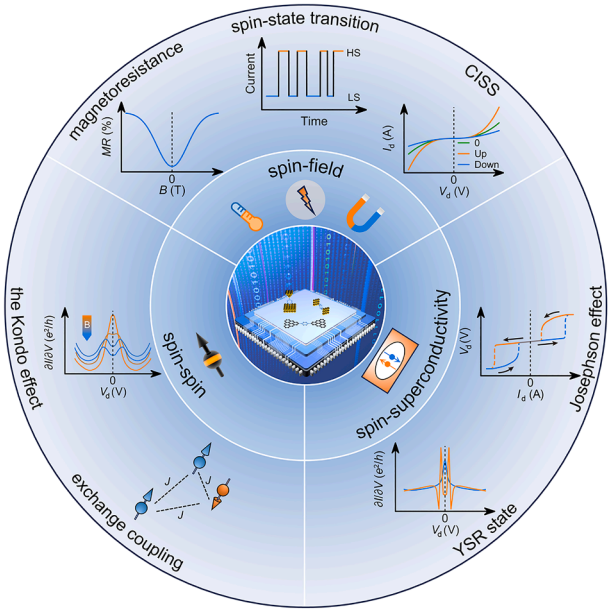

Figure 1. Molecular-scale spin interactions, including spin-spin, spin-field, and spin-superconductivity interactions

Spin-spin interactions—such as exchange coupling and the Kondo effect—demonstrate how molecular spins interact to produce distinctive transport behaviors. Spin-field interactions highlight the control of spin states by electric and magnetic fields within molecular junctions. Spin-superconducting interactions reveal emergent quantum phenomena at the interface between the spins and superconducting electrodes, including Yu-Shiba-Rusinov (YSR) states and single-molecule Josephson junction effects.

and control of quantum spin effects, such as exchange coupling, Kondo resonance, and spin blockade.[17–20] Furthermore, recent advances have integrated electron spin resonance (ESR) with these platforms,[21–23] enabling coherent manipulation of molecular spins and propelling molecular quantum computing.

Despite these advancements, critical challenges persist. Reliable control of spin states at room temperature is hindered by decoherence effects, while the integration of molecular spins into a device architecture is often limited by interfacial spin scattering and magnetic quenching, which compromise the device performance.[12,24] Addressing these challenges requires a multidisciplinary approach that bridges molecular engineering, nanofabrication, and quantum theory to decode spin interaction mechanisms and translate them into functional quantum technologies.

In this review, we present a structured overview of molecular-scale spin effects, focusing on three principal interaction types: spin-spin, spin-field, and spin-superconductivity interactions (Figure 1). We analyze the primary mechanisms within each category, supported by recent advances, to illustrate how these interactions shape molecular spin behaviors and contribute to device functionalities. By integrating these perspectives, we highlight both current achievements and the challenges that remain in leveraging molecular spin effects for quantum-enabled technologies.

SPIN-SPIN INTERACTIONS

Spin-spin interactions in molecular systems are generally governed by two key phenomena: exchange coupling between localized spins and the Kondo effect originating from spin-conduction electron interactions. In this section, we will dissect these mechanisms and their implications for spin manipulation.

Exchange coupling

Exchange coupling refers to the quantum mechanical interaction between the spins of two or more particles (typically electrons), leading to the alignment (ferromagnetism) or anti-alignment (antiferromagnetism) of their magnetic moments. This coupling arises from the Pauli exclusion principle and Coulomb repulsion, which dictate electron-spin interactions based on spatial proximity and quantum states.

In molecular-scale spintronics, exchange coupling fundamentally defines the magnetic and quantum behaviors of nanostructures, influencing phenomena such as the stability of magnetic states and overall spin dynamics.[25–27] For instance, antiferromagnetic atomic chains can be constructed by systematically assembling Fe atoms on a Cu_2N surface using a low-temperature STM (Figure 2A).[17] Adjacent atoms exhibit antiferromagnetic coupling (J = 1.2 meV), forming linear atomic chains with two distinct Néel states. Remarkably, the thermal switching rate between these states remains temperature independent below 5 K, suggesting quantum tunneling of magnetization. Reducing quantum tunneling can be achieved through exchange coupling between two chains, as shown in Figure 2B. Although the exchange coupling between the two chains (J' = 0.03 meV) is much weaker than the intra-chain exchange coupling, it significantly suppresses tunneling (Figure 2C). This large difference between J and J', attributed to the crystal structure of the Cu_2N surface, supports the presence of superexchange-mediated interactions within the Cu_2N molecular network.

Beyond static systems, exchange coupling enables dynamic spin control.[28] By using an STM-based electronic pump-probe spectroscopy to measure the spin relaxation time of an Fe trimer (Figure 2D), researchers can adjust the exchange coupling between the tip and nanomagnet by varying the tip-sample distance. Notably, the spin relaxation times of the central and terminal Fe atoms exhibit opposite trends as the tip-sample distance, and thus the exchange coupling strength is varied (Figure 2E). This precise manipulation, enabled by a Heisenberg exchange interaction, emphasizes the value of exchange coupling as a tool for controlling quantum states in molecular spintronic devices.

Exchange coupling also provides a tunable mechanism for controlling spin-state transitions and electron transport. A notable example involves embedding a diradical molecule in a three-terminal single-molecule junction,[29] where an applied gate voltage induces reversible redox-state changes (Figures 2F and 2G). Inelastic electron tunneling spectroscopies for the two stable redox states reveal that the added electron undergoes exchange coupling with the two radical spins, transforming the molecular magnetic state from a singlet to a doublet with three unpaired electrons while maintaining an open-shell configuration.

Please cite this article in press as: Yang et al., Mechanisms and control of spin interactions in molecular-scale spintronics, Newton (2025), https://doi.org/10.1016/j.newton.2025.100170

CellPress
OPEN ACCESS

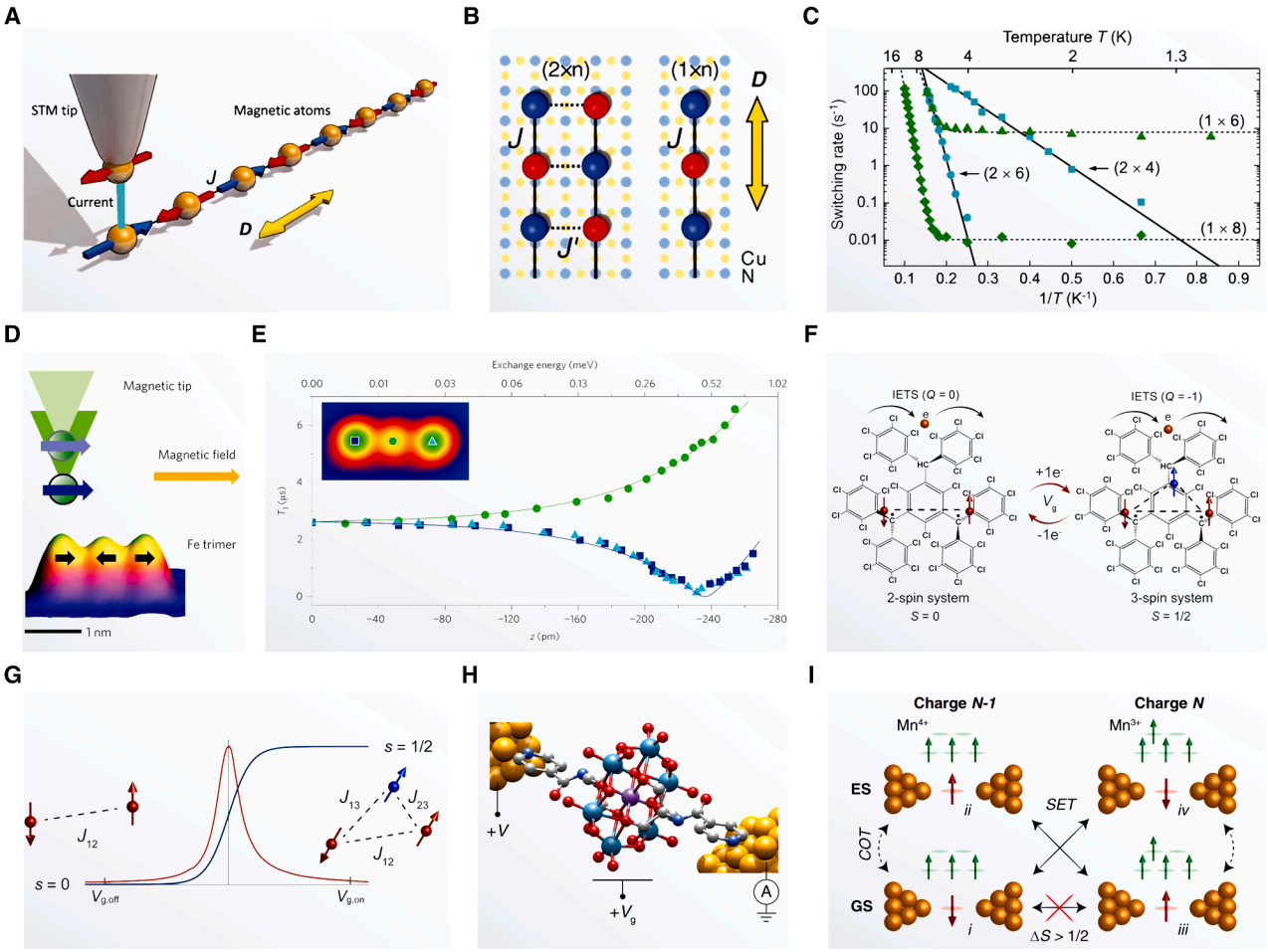

Figure 2. Exchange coupling at the atomic or molecular scale

(A) Schematic of an Fe chain on the Cu_2N surface coupled antiferromagnetically with exchange energy J. Reprinted, with permission, from Loth et al.[17] Copyright 2012, American Association for the Advancement of Science.

(B) Schematic of Fe chains in different arrays ($2 \times n$ and $1 \times n$) on Cu_2N substrates. Yellow and light-blue circles represent Cu and N atoms, respectively. Red and blue balls denote Néel states with spin orientations parallel and antiparallel to the tip spin. Reprinted, with permission, from Loth et al.[17] Copyright 2012, American Association for the Advancement of Science.

(C) Arrhenius plots of the switching rates for different arrays (1×6, 1×8, 2×4, and 2×6). Reprinted, with permission, from Loth et al.[17] Copyright 2012, American Association for the Advancement of Science.

(D) Schematic of exchange coupling between a magnetic STM tip and an Fe trimer dependent on the tip-sample distance. The black arrows indicate spin orientations of Fe atoms. The gray and blue arrows represent spin orientations of the magnetic tip at larger and smaller tip-sample distances. Reprinted, with permission, from Yan et al.[28] Copyright 2015, Springer Nature.

(E) Spin relaxation time (T_1) of the Fe trimer as a function of tip position (z). Symbols are experimental data measured on individual Fe atoms, and solid lines are the calculated dependence of T_1. Reprinted, with permission, from Yan et al.[28] Copyright 2015, Springer Nature.

(F) Structure and magnetism schematics of the neutral and reduced forms of 2,4,6-hexakis-(pentachlorophenyl)mesitylene diradical molecule. Reprinted, with permission, from Gaudenzi et al.[29] Copyright 2017, American Chemical Society.

(G) Differential conductance (red) and spin value s (blue) of different redox centers as a function of V_g. Reprinted, with permission, from Gaudenzi et al.[29] Copyright 2017, American Chemical Society.

(H) Sketch of the pyridine-functionalized Mn(III) Anderson polyoxometalate molecule, gold electrodes, and measurement circuit. Reprinted, with permission, from de Bruijckere et al.[18] Copyright 2019, American Physical Society.

(I) Electron configurations of Mn(III) Anderson polyoxometalate molecule under different charge and spin states. The green and red arrows denote spin orientations of the center metal and the ligand. Reprinted, with permission, from de Bruijckere et al.[18] Copyright 2019, American Physical Society.

In addition, chemical design can harness exchange coupling to control quantum transport. For instance, pyridine-functionalized Mn(III) Anderson polyoxometalate molecules (Figure 2H) exhibit charge-induced magnetic phase transitions.[18] When the molecule is charged, the added charge not only increases the inherent spin but also changes the exchange coupling from antiferromagnetic to ferromagnetic, raising the total spin by 1 (Figure 2I). The ground-state spins of different charge states

are 1 and 5/2, respectively, with a spin difference of 3/2. Following spin-selection rules, single-electron tunneling between these states is forbidden, leading to the ground state spin blockade (GSSB). Applying a strong magnetic field shifts the high-spin state to the oxidized state, reducing the spin difference to 1/2, thereby lifting the GSSB. This experiment illustrates how exchange coupling regulates electron transport via spin-selection rules and demonstrates charge-induced magnetic phase transitions in high-spin devices, effectively suppressing resonant transport.

The Kondo effect

The Kondo effect is a prominent phenomenon related to the role of spin in electron transport, manifesting as anomalous conductance near zero bias. The discovery of this effect originated from the counterintuitive observation that the electrical resistance of certain metals increases at low temperatures.[30,31] In 1964, Jun Kondo proposed that this behavior arises from enhanced scattering due to magnetic impurities.[32] Specifically, conduction electrons form a surrounding cloud that screens the impurity's magnetic moment, thereby increasing the scattering of electrons near the Fermi level—a phenomenon now known as the Kondo effect. This effect has been widely studied in nanoscale systems with net spin, where it arises from the coupling between a localized spin and the spins of conduction electrons, forming a many-body spin state, commonly referred to as the Kondo screening cloud,[33] as shown in Figure 3A. This phenomenon is intrinsically rooted in the Pauli exclusion principle and strong electron-electron repulsion.[34] As temperature increases, the Kondo effect correlates with high-order transport processes, resulting in a gradual broadening of the resonance peak with pronounced temperature dependence. Applying a magnetic field lifts the spin degeneracy of the Kondo resonance, leading to Zeeman splitting. Temperature and magnetic field dependencies of Kondo resonance thus effectively characterize electron spin properties during transport while highlighting quantum transport properties in molecular systems.

Early reports of the Kondo effect can be traced back to studies on magnetic single-molecule transistors, where the differential conductance (d*I*/d*V*) measurements revealed a distinct Kondo resonance peak near zero bias.[19,20] Through single-molecule electromigration junctions, the studies have demonstrated that the gate voltage can effectively modulate charge and spin states in molecules, thereby controlling the Kondo resonance effect (Figure 3B). The length of the molecular system also dictates whether Coulomb blockade or Kondo resonance predominates (Figure 3C). Inspired by these works, the Kondo effect has also been extensively studied in various regulations.[39,40] One notable study is to measure Kondo-assisted tunneling using C_{60}-based single-molecule break junctions with ferromagnetic nickel electrodes.[41] Another is to utilize MCBJs to stretch molecules, altering their symmetry and enabling manipulation of molecular spin states without applying a magnetic field,[35] as shown in Figure 3D. With the deepening exploration of Kondo effect modulation, it has emerged as a powerful spectroscopic tool for identifying molecular states exhibiting a non-zero net spin.[42–44]

In a recent work, Köbke et al.[36] used STM to investigate a ligand-strapped Ni-porphyrin molecule, demonstrating reversible switching between high-spin and low-spin states through Kondo resonance modulation (Figure 3E). This study highlighted the magnetic bistability through the presence or absence of a Kondo resonance, validating a novel concept for ligand-strapped single-molecule spin switches with differential conductance spectroscopy. The results illustrated the reversible interlocking of spin and coordination states through electron injection, advancing our understanding of spin-state control in molecular systems.

In addition to magnetic metal complex systems, the Kondo effect has also been studied in individual radical molecules.[37] For example, polychlorotriphenylmethyl (PTM) molecules, integrated into single-molecule devices, exhibited Kondo anomalies associated with paramagnetism (Figure 3F). Experiments involving temperature and magnetic field variations confirmed the stability of this Kondo anomaly and identified the origins of the magnetism. Moreover, another study reported the evolution and universality of the two-stage Kondo effect in a single-molecule transistor,[38] as shown in Figures 3G and 3H. The Kondo resonance effect exhibited universal patterns across tunable parameters such as temperature, magnetic field, and bias voltages, showcasing its quadratic dependence. The Kondo effect thus offers profound insights into spintronic properties at the molecular level and enhances our understanding of spin interactions, which are also related to magnetoresistance and superconductivity, topics we will explore in subsequent sections.

SPIN-FIELD INTERACTIONS

The interaction between molecular spins and external fields provides a versatile tool for controlling spin states and enabling functional devices. This section explores three pivotal phenomena: spin-state transitions induced by field perturbations, magnetoresistance in spin-dependent transport, and chirality-induced spin selectivity (CISS) in chiral molecular systems.

Spin-state transitions

Spin-state transitions are fundamental for dynamically controlling spin configurations at the molecular or atomic level. Recent advances have demonstrated that external fields, such as electric and magnetic fields, can modulate spin states in single-molecule systems.[45–48] This ability to control spin states holds significant promise for quantum information processing and spin-based devices.[9,13] Several studies have examined innovative approaches to harness these transitions, providing insights into governing the spin-state dynamics.

A remarkable study by Thiele et al.[49] introduced the use of the hyperfine Stark effect as an atomic-scale magnetic field transducer, achieving electric-driven nuclear spin resonance in SMMs (Figure 4A). Using a $TbPc_2$ single-molecule magnet, coupled to source, drain, and gate electrodes, they applied microwave pulses to modulate the hyperfine constant, inducing magnetic field oscillations that enabled coherent nuclear spin qubit manipulation (Figure 4B).

Beyond hyperfine interactions, methods for measuring single-molecule entropy have also proven valuable for understanding spin-state transitions.[50,52,53] For instance, using an individual nitronyl nitroxide radical (Figure 4C), thermocurrent spectroscopy

Please cite this article in press as: Yang et al., Mechanisms and control of spin interactions in molecular-scale spintronics, Newton (2025), https://doi.org/10.1016/j.newton.2025.100170

CellPress
OPEN ACCESS

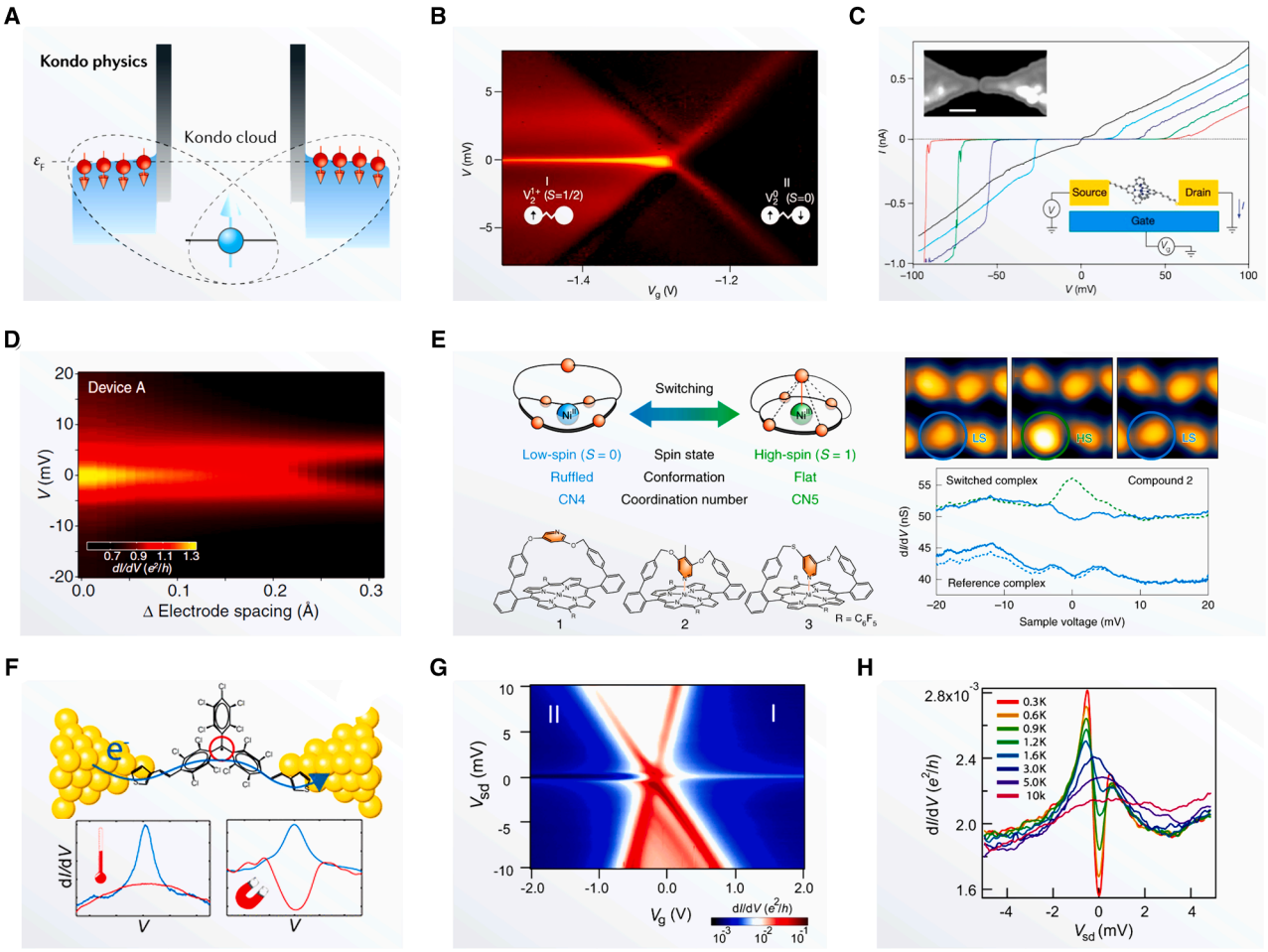

Figure 3. The Kondo effect and related phenomena in single-molecule junctions

(A) The Kondo effect arises from the formation of a many-body spin singlet state between the spins on the molecule and the conducting electrons, leading to the establishment of a "Kondo screening cloud." Reprinted, with permission, from Gehring et al.[33] Copyright 2019, Springer Nature.

(B) d*I*/d*V* plots obtained from the single-molecule transistor containing an individual divanadium molecule, demonstrating the influence of gate voltage on the spin behavior through the Kondo effect. Reprinted, with permission, from Liang et al.[19] Copyright 2002, Springer Nature.

(C) *I*-*V* curves of a single-electron transistor containing cobalt complexes at various V_g. The upper inset features a topographic atomic force microscope (AFM) image of the electrodes, highlighting the gap (scale bar, 100 nm). The lower inset provides a schematic representation of the device. Reprinted, with permission, from Park et al.[20] Copyright 2002, Springer Nature.

(D) d*I*/d*V* plots of a Co spin-crossover single-molecule junction fabricated via the MCBJ method, demonstrating the splitting of the Kondo peaks as a function of bias voltage and mechanical stretching. Reprinted, with permission, from Parks et al.[35] Copyright 2010, American Association for the Advancement of Science.

(E) Reversible spin-state switching of complexes 1–3 on Ag(111) is demonstrated through topographs showing complex 2 transitioning between low-spin and high-spin states, validated by the Kondo effect. Reprinted, with permission, from Köbke et al.[36] Copyright 2019, Springer Nature.

(F) Schematic diagram illustrating MCBJ-based single-molecule junctions involving free radicals, along with the temperature and magnetic field modulation of their Kondo effect. Reprinted, with permission, from Frisenda et al.[37] Copyright 2015, American Chemical Society.

(G) d*I*/d*V* plots showing the second-order Kondo resonance effect of MnPc molecular junctions under different gate voltages at 280 mK. Reprinted, with permission, from Guo et al.[38] Copyright 2021, Springer Nature.

(H) d*I*/d*V* curves showing the two-stage Kondo effect of MnPc molecular junctions at $V_g = -2$ V and various temperatures. Reprinted, with permission, from Guo et al.[38] Copyright 2021, Springer Nature.

detected transitions between singlet and triplet states across different redox states. The molecule's neutral state displayed a doublet ground state with an unpaired electron, while the reduced state exhibited a singlet ground state (Figure 4D). Importantly, upon applying an external magnetic field, a low-lying triplet excited state emerged in the reduced molecule. This approach allowed quantification of entropy changes associated with spin-state transitions, illustrating the role of external fields in state modulation.

Building on these insights, Yang et al.[51] proposed a method to regulate quantum spin transitions in a single diradical molecule at room temperature (Figures 4E and 4F). By monitoring real-time current in a single-molecule junction, they observed transitions from closed-shell to open-shell configurations modulated

Please cite this article in press as: Yang et al., Mechanisms and control of spin interactions in molecular-scale spintronics, Newton (2025), https://doi.org/10.1016/j.newton.2025.100170

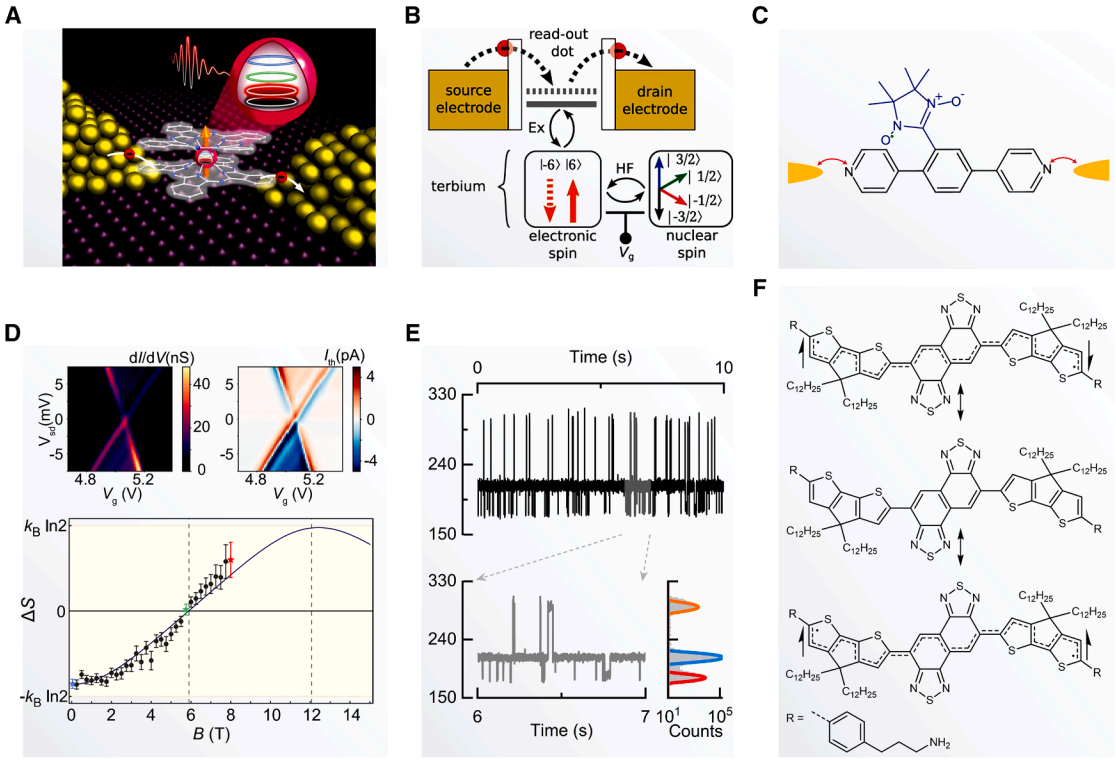

Figure 4. Spin-state transitions in single-molecule devices

(A) Schematic of a nuclear spin qubit transistor based on a single $TbPc_2$ molecular magnet. The four anisotropic nuclear spin states of Tb^{3+} (colored circles) can be manipulated via an electric field pulse. Reprinted, with permission, from Thiele et al.[49] Copyright 2014, American Association for the Advancement of Science.

(B) Three coupled subsystems of the nuclear spin qubit transistor mediated by the hyperfine coupling and antiferromagnetic exchange coupling. Reprinted, with permission, from Thiele et al.[49] Copyright 2014, American Association for the Advancement of Science.

(C) Sketch of a radical molecule with a nitronyl nitroxide side group connected to source and drain electrodes. The red arrows indicate electron tunneling on and off the radical molecule. Reprinted, with permission, from Pyurbeeva et al.[50] Copyright 2021, American Chemical Society.

(D) Bias and gate voltage-dependent differential conductance (top left) and thermocurrent (top right), and entropy change as a function of the magnetic field strength (bottom) of a single-molecule junction in (C). Error bars are the fitting errors and the limitations of the fitting equations explained in Pyurbeeva et al.[50] Reprinted, with permission, from Pyurbeeva et al.[50] Copyright 2021, American Chemical Society.

(E) Real-time current detection for quantum spin transitions of individual diradical molecules. Conductance states (blue, yellow, and red Gaussian fits) correspond to closed-shell singlet, open-shell singlet, and open-shell triplet configurations of the diradical. Reprinted, with permission, from Yang et al.[51] Copyright 2024, Springer Nature.

(F) Resonant structural transitions between closed-shell and open-shell forms of the diradical molecule. Reprinted, with permission, from Yang et al.[51] Copyright 2024, Springer Nature.

by temperature, bias voltage, and magnetic fields. Specifically, applying an electric field reduced the potential energy gap between the closed-shell singlet and open-shell triplet states, facilitating the transition. Similarly, an increase in magnetic field strength promoted the transition to the triplet state. These findings emphasized the critical role of spin-state transitions in quantum thermodynamics and offer new methods for characterizing spin behavior in molecular systems, although stable manipulation of quantum spin states at room temperature remains a significant challenge.

Magnetoresistance

Magnetoresistance (MR) is the change in electrical resistance when a magnetic field is applied, commonly defined by MR = $([R_B - R_0]/R_0) \times 100\%$, where R_B and R_0 are resistances with and without a magnetic field, respectively. MR has important applications in hard disk drives and magnetoresistive memory, and research into MR at the molecular scale is increasing as the demand for higher storage densities grows.[54,55] The focus in molecular MR research is the interplay between magnetic fields, molecular structure, and spin-polarized transport. Investigations often encompass two main types: magnetic molecules with intrinsic spins and non-magnetic molecules paired with magnetic electrodes.

A critical factor governing MR in both molecular and macroscopic systems is the spin-dependent hybridization at the molecule-electrode interface. This phenomenon, termed the "spinterface" effect,[56,57] arises when molecular orbitals hybridize with spin-split electronic states of ferromagnetic electrodes. The spinterface mechanism, first demonstrated in molecular layers on ferromagnetic substrates,[56] induces spin-polarized broadening of molecular energy levels and creates spin-selective

Please cite this article in press as: Yang et al., Mechanisms and control of spin interactions in molecular-scale spintronics, Newton (2025), https://doi.org/10.1016/j.newton.2025.100170

transport pathways. In single-molecule devices, this effect enables precise control over spin-dependent transport by aligning molecular orbitals with the spin-polarized density of states of electrodes.

In magnetic molecular systems, MR arises from field-dependent spin and orbital interactions. A striking example is the Dy@C_{84}-based single-molecule transistor, which exhibits giant MR (1,100%) under specific electric fields (Figures 5A and 5B).[58] This effect arises from the metal-cage hybridization within the fullerene, where an increased magnetic field reduces orbital overlap and hybridization density. According to the Landauer model, the resulting decrease in density of states lowers current, thereby enhancing MR.

The interplay between MR and the Kondo effect reveals how spin interactions govern transport. In PTM radical molecular junctions formed using MCBJs,[59] the high MR results from spin-dependent scattering at the metal-molecule interface, while the Kondo effect arises from unpaired spins in the asymmetrically coupled molecule center (Figures 5C and 5D). Notably, molecular junctions with strong Kondo resonance display reduced MR, whereas more symmetric junctions, which lack significant Kondo effects, exhibit higher MR. In addition, MR can be tuned by mechanically stretching the junction. This interaction underscores the crucial role of molecular coupling symmetry in modulating both spin and charge transport at the molecular scale.

Magnetic anisotropy and multi-orbital effects further enrich MR mechanisms. In Fe phthalocyanine,[60] a magnetic field can modulate electron transport pathways between two distinct molecular orbitals, leading to anisotropic magnetoresistance (AMR) of up to 93%. At zero magnetic field, electron transport is dominated by Kondo resonance scattering through the $d\pi$ orbital. However, at higher magnetic fields, the electron transmission shifts to the dz^2 orbital, with an intermediate field inducing transport through both orbitals (Figure 5E). This orbital-selective MR demonstrates how molecular design can harness magnetic anisotropy for tunable spintronic devices.

For non-magnetic molecules paired with magnetic electrodes, MR depends on the relative alignment of electrode spins. Crucially, the induction of spin polarization in molecules at ferromagnetic interfaces is a universal phenomenon, independent of the device scale.[12,63] For instance, in Alq_3 molecules hybridized with magnetic surfaces,[64,65] interfacial exchange coupling induces spin-polarized empty states near the Fermi level, facilitating efficient spin injection despite the absence of intrinsic molecular magnetism.

In hydrogen phthalocyanine molecules positioned between a cobalt-coated tungsten tip and cobalt nanoislands on a Cu (111) surface, distinct conductance and MR differences arise, depending on whether the spins in the tip and substrate are aligned parallel or antiparallel (Figure 5F).[61] This effect is driven by spinterface-mediated spin-dependent hybridization between molecular orbitals near the Fermi level and the electronic states of magnetic electrodes.

Similarly, Fe-terephthalic acid (TPA)-Fe single-molecule junctions exhibit AMR that increases as the magnetic field strength increases or bias voltage decreases (Figures 5G and 5H).[62] Here, the altering magnetic orientation of Fe electrodes modifies electronic coupling at the TPA-Fe interface, directly affecting the probability of electron tunneling. These findings illustrate that even simple non-magnetic molecules can exhibit substantial MR effects when coupled with magnetic electrodes, emphasizing the role of spinterface in controlling spin transport.

Chirality-induced spin selectivity

CISS enables non-magnetic chiral molecules to filter electron spins through structural chirality—a capability previously exclusive to inorganic ferromagnetic materials.[15,16] Since its discovery in 1999,[66] CISS has been observed in diverse systems including DNA,[67,68] oligopeptides,[69,70] helicenes,[71,72] and organic-inorganic hybrid materials.[73,74] One of the fundamental methods for observing CISS is contact-based measurements of spin transport, whereby altering the magnetic state of a contact (either a substrate or tip) changes the current transmitted through the molecule.[16] This approach is widely used due to its straightforward design, avoiding complex spectroscopic setups and simplifying data analysis.

DNA exemplifies how the molecular geometry governs the CISS effect. In hybridized nanoparticle-double-stranded DNA (dsDNA)-nickel complexes on a nickel substrate (Figure 6A), spin-dependent conductivity studies revealed that longer dsDNA oligomers (40 and 50 bp) exhibited significantly higher spin selectivity than shorter ones (26 bp).[67] This difference is attributed to the larger effective barrier in longer molecules, which preferentially suppresses currents of unfavorable spin orientations (Figure 6B). Importantly, this level of spin selectivity could not be fully explained by SOC, as the effective energy gap between the two spin states, approximately 1 eV, is much larger than spin-orbit interactions typically observed in carbon-based molecules.

In another study, Torres-Cavanillas et al.[69] explored CISS in self-assembled monolayers of helical lanthanide-binding peptides (Figures 6C and 6D). Using cyclic voltammetry, electrochemical impedance spectroscopy, and solid-state devices using liquid-metal drop contacts, the researchers demonstrated that paramagnetic centers in these molecules significantly enhanced spin filtering. These findings underscored the crucial role of paramagnetic centers in amplifying spin polarization in chiral molecular systems.

In addition, Safari et al.[71] employed spin-polarized STM at 5 K to investigate enantiomers of helicene molecules adsorbed on a ferromagnetic cobalt surface (Figure 6E). Their results revealed a magnetochiral conductance asymmetry of up to 50%, observed when either the molecular chirality or the magnetization direction of the STM tip or cobalt substrate was reversed. This study ruled out ensemble effects due to electron-phonon coupling or intermolecular interactions as the primary mechanism behind CISS, confirming that the effect is an intrinsic property of chiral molecules.

In an innovative application of CISS to reaction monitoring, Yang et al.[75] tracked stereochemical changes in real time during the Michael addition reaction (Figure 6F). By constructing a single-molecule spin valve device, they quantified the voltage-dependent response of different enantiomers and observed that the CISS effect gradually diminished as temperature increased. This observation supports the spinterface mechanism, which attributes CISS to spin-torque interactions between

Please cite this article in press as: Yang et al., Mechanisms and control of spin interactions in molecular-scale spintronics, Newton (2025), https://doi.org/10.1016/j.newton.2025.100170

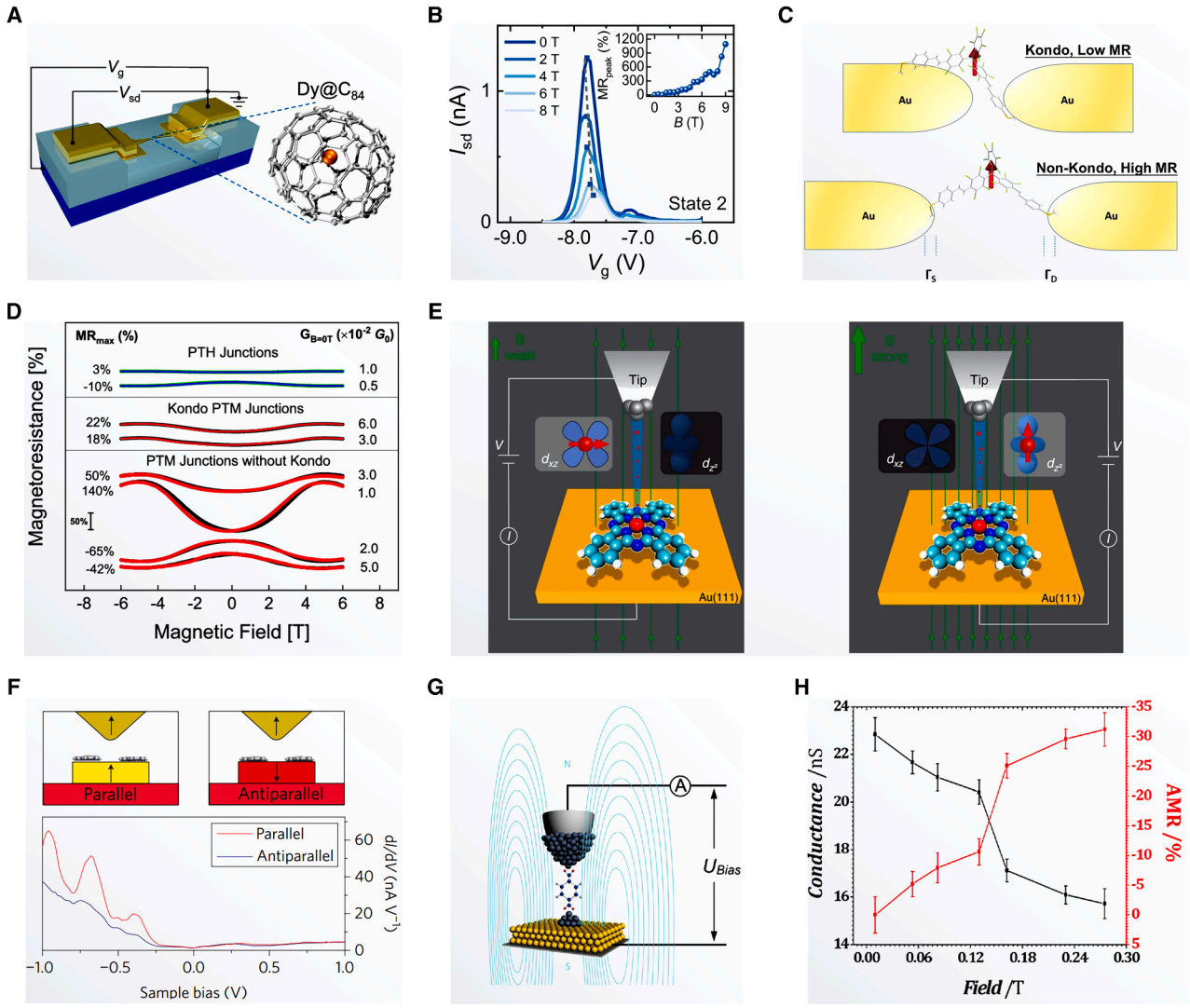

Figure 5. MR effects in single-molecule junctions

(A) Schematic of a three-terminal Dy@C_{84} single-molecule transistor and the structure of Dy@C_{84}. Reprinted, with permission, from Wang et al.[58] Copyright 2024, Springer Nature.

(B) Variation of the resonant tunneling peaks with magnetic field for a specific molecular state at V_{sd} = 5 mV. The inset shows the magnetic field dependence of MR, which is up to 1,100% at 9 T. Reprinted, with permission, from Wang et al.[58] Copyright 2024, Springer Nature.

(C) An illustration of different configurations of PTM junctions and corresponding Kondo resonance or MR. Asymmetric junctions induce Kondo resonance, while symmetric configurations enable the high MR. Reprinted, with permission, from Hayakawa et al.[59] Copyright 2016, American Chemical Society.

(D) MR measurements on different single-molecule junctions of PTM and PTH measured at 4.2 K with a bias of 30 mV. Reprinted, with permission, from Hayakawa et al.[59] Copyright 2016, American Chemical Society.

(E) Schematics of the electron transport process through an STM junction with Fe phthalocyanine molecules absorbed on a Au(111) surface at different magnetic fields. Left panel (weak magnetic field): Fe spins are oriented in-plane, and current tunnels through the d_{xz}/d_{yz} orbital. Right panel (strong magnetic field): Fe spins align with the magnetic field, and electrons predominantly tunnel via the d_{z^2} orbital. Reprinted, with permission, from Yang et al.[60] Copyright 2019, Springer Nature.

(F) Typical d*I*/d*V* spectra of a hydrogen phthalocyanine molecule on parallel and antiparallel oriented cobalt islands. Reprinted, with permission, from Schmaus et al.[61] Copyright 2011, Springer Nature.

(G) Schematic of Fe-TPA-Fe single-molecule junctions under a magnetic field. Reprinted, with permission, from Li et al.[62] Copyright 2015, American Chemical Society.

(H) Variations of the conductance and AMR of a single Fe-TPA-Fe molecule with a parallel magnetic field strength at a bias of −0.1 V. Error bars are the standard deviations of five measurements. Reprinted, with permission, from Li et al.[62] Copyright 2015, American Chemical Society.

Please cite this article in press as: Yang et al., Mechanisms and control of spin interactions in molecular-scale spintronics, Newton (2025), https://doi.org/10.1016/j.newton.2025.100170

CellPress
OPEN ACCESS

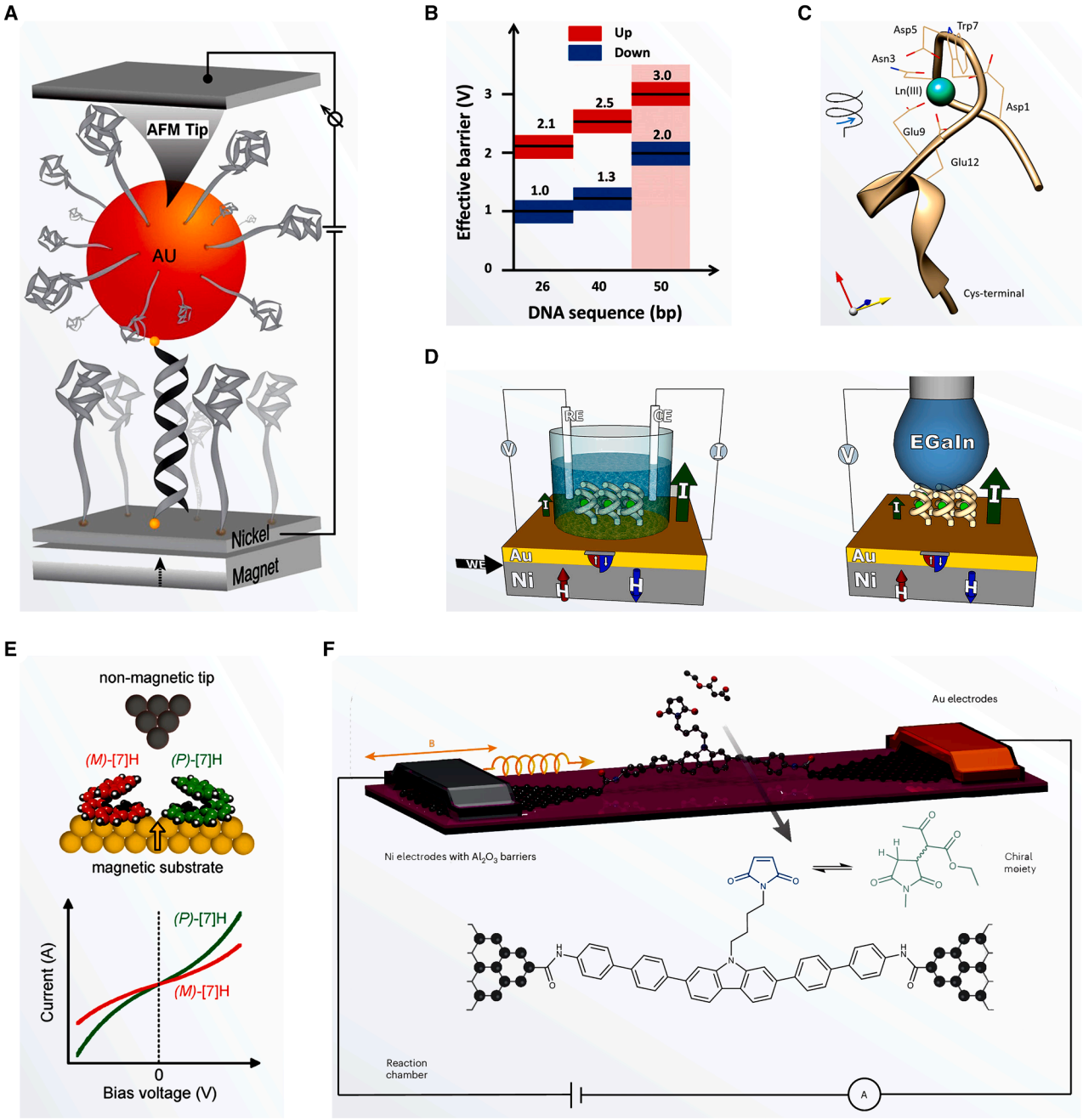

Figure 6. CISS effects in molecular junctions

(A) Self-assembled monolayer of ssDNA between the nickel substrate and the tip of the atomic force microscope (AFM) for the measurement of spin-specific electron conduction. Reprinted, with permission, from Xie et al.[67] Copyright 2011, American Chemical Society.

(B) Effective barrier for the three DNA oligomers (26, 40, and 50 bp) studied when the magnet is pointing down (blue) or up (red). The absolute value of the barrier increases with increasing the DNA length, while the barrier gap between spins of different orientations is independent on their length. Error bars are the uncertainties (±0.2 V) of the effective band gaps. Reprinted, with permission, from Xie et al.[67] Copyright 2011, American Chemical Society.

(C) Structure of the helical metallopeptide used for spin-filtering studies. Reprinted, with permission, from Torres-Cavanillas et al.[69] Copyright 2020, American Chemical Society.

(D) Schematic of three-electrode electrochemical cell (left) and liquid-metal EGaIn device (right) for spin-dependent measurements of self-assembled monolayers of helical metallopeptides. Reprinted, with permission, from Torres-Cavanillas et al.[69] Copyright 2020, American Chemical Society.

(legend continued on next page)

the spin imbalance in chiral molecules and the surface magnetization of metallic electrodes.

However, the physical origin of CISS remains actively debated, with multiple competing hypotheses under investigation. Early theoretical models emphasized SOC, but experimental spin-dependent energy scales far exceed intrinsic SOC values of light organic elements.[15,76] This discrepancy has driven proposals for enhanced effective SOC through introducing various factors into theoretical models. Meanwhile, temperature-activated polarization in systems like dsDNA and chiral quartz crystals suggests contributions from electron-phonon interactions or chiral phonons.[77,78] Recent studies also implicate that orbital polarization effects,[79,80] assisted by the strong SOC of metallic electrodes, can induce spin polarization, enabling CISS-driven magnetoresistance and spin-valve effects. Collectively, these studies highlight that CISS likely arises from a confluence of mechanisms—spanning molecular chirality, vibrational dynamics, and interfacial SOC—with their relative dominance dependent on system-specific conditions.

SPIN-SUPERCONDUCTIVITY INTERACTIONS

The interaction between spin and superconductivity has emerged as a frontier topic in spintronics,[81] where understanding the interplay between Cooper pairs in superconducting electrodes and the physical properties of conducting molecules is essential for developing superconducting spintronic devices. When magnetic atoms or molecules are coupled to the superconductor interface, they introduce a scattering potential for quasiparticles in the substrate, leading to the formation of bound states commonly referred to as Yu-Shiba-Rusinov (YSR) states.[82–84] In this section, we explore how molecular systems serve as versatile platforms to probe these interactions, with a particular focus on three key themes: (1) the competition between Kondo screening and superconductivity; (2) the engineering of multiple YSR states; and (3) superconductivity-enabled spin control.

A key breakthrough in this field was the observation of the Josephson junction effect at the single-molecule level in C_{60}-based transistors,[85] as illustrated in Figures 7A and 7B. By engineering devices with varying Kondo coupling strengths, researchers revealed that superconductivity disrupts the Kondo peak in the weak coupling regime. This indicates a coexistence and competition among Coulomb repulsion, the Kondo effect, and superconductivity under gate control conditions.

Notably, the Kondo effect arises from the interaction between molecular spins and the conduction electrons of the electrodes, while the conduction electrons in the superconducting electrodes tend to form Cooper pairs, leading to competition between the two phenomena. When the Kondo coupling is weak, Cooper pairs in the electrodes suppress the Kondo effect, allowing only YSR states to be observed instead of Kondo resonance peaks. In 2011, Franke et al.[86] utilized STM to probe manganese-phthalocyanine (MnPc) molecules on a Pb(111) surface. They observed spatial variations in Kondo resonance and YSR states, directly linking molecular adsorption geometry to the quantum phase transition between singlet and doublet states (Figure 7C). These studies laid a solid foundation for exploring the interplay between the Kondo effect and YSR states within molecular systems, enabling further research into multiple YSR systems.

The origins of multiple YSR states within the superconducting gap are influenced by mechanisms such as magnetic anisotropy and SOC.[87,88] For instance, in the MnPc/Pb(111) system, magnetic anisotropy splits the $S = 1$ spin state into three energy levels, generating three pairs of YSR states (Figure 7D).[87] Similarly, SOC in the molecular magnet Tb_2Pc_3 on Pb(111) (Figure 7E) led to YSR sub-band states.[88] The two pairs of YSR states arose from the splitting of the lowest unoccupied molecular orbital and charge fluctuations, demonstrating that the system corresponds to a weakly coupled double-impurity YSR model within a single molecule.

Moreover, applying superconducting characteristics to the study of intrinsic properties of molecules is of paramount importance. For example, superconducting gaps can protect molecular spin states and excitations without decay for several microseconds by limiting electronic states near the superconductor Fermi level, preventing energy relaxation into the substrate,[89] as shown in Figure 7F. This phenomenon provides a platform for quantum information processing based on molecular magnets and enables excitation and readout of spins on superconducting substrates. In addition, the proximity effect of superconductors can effectively probe the transport properties of molecules.[91,92] Intriguingly, non-magnetic chiral molecules, such as chiral alpha-helical polypeptide molecules on $NdSe_2$, induce YSR-like states on superconducting surfaces.[93] Another study reported that the Kondo effect can be reversibly turned on and off using a superconducting Nb tip.[94] By adjusting the tip-sample distance at low temperatures, a reversible switch between the Kondo dip and inelastic electron tunneling was achieved. When the tip picked up the molecule, the Kondo dip transitioned into a YSR state within the superconducting gap, offering a new approach for controlling the Kondo effect in single-molecule junctions.

Recent advancements in nanostructured superconductors focus on atomic-level control. Single-atom Josephson junctions have been fabricated and utilized to investigate non-reciprocal charge-transport processes in diodes.[90] As shown in Figure 7G, three different atomic junctions—Pb, Cr, and Mn—demonstrated the asymmetry of current modulation through junction conductivity, with the sign of the asymmetry depending on the type of atom used. This work integrated atomic-scale Josephson junctions with single-atom manipulation to explore the ultimate limits of superconducting junction miniaturization. Collectively, these investigations into the complex

(E) Magnetochiral conductance measurements based on the spin-polarized STM, with the enantiomer of heptahelicene molecules on a ferromagnetic surface exhibiting different conductance. Reprinted, with permission, from Safari et al.[71] Copyright 2024, Wiley-VCH GmbH.
(F) Schematic of a single-molecule spin-valve device for monitoring the Michael addition reaction. Nickel electrodes enable spin-polarized injection, with *in situ* electrical measurements during the reaction. Reprinted, with permission, from Yang et al.[75] Copyright 2023, Springer Nature.

Please cite this article in press as: Yang et al., Mechanisms and control of spin interactions in molecular-scale spintronics, Newton (2025), https://doi.org/10.1016/j.newton.2025.100170

CellPress
OPEN ACCESS

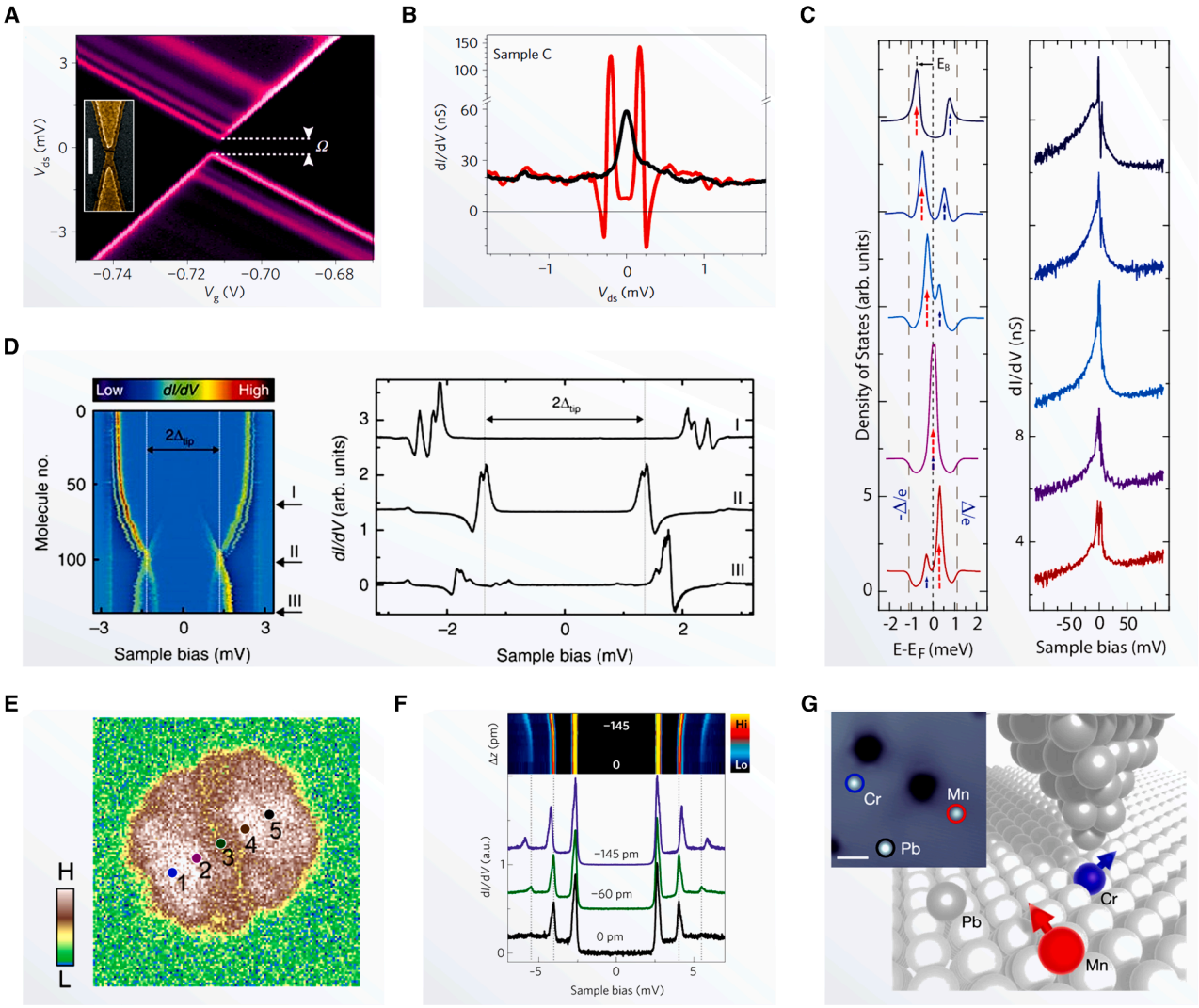

Figure 7. The interplay between spin and superconductivity

(A) d*I*/d*V* plots of a C_{60} single-molecule junction in the weak-coupling limit. The inset shows an SEM image of an aluminum nanogap created by electromigration (scale bar, 300 nm), measured at zero magnetic field and T = 35 mK. Reprinted, with permission, from Winkelmann et al.[85] Copyright 2009, Springer Nature.

(B) Data illustrating the normal (black line) and superconducting (red line) states. In sample C with a Kondo temperature (T_K) of 0.7 K, the onset of superconductivity suppresses the Kondo resonance. Sample C represents a C_{60} single-molecule device in which superconductivity suppresses the Kondo resonance. Reprinted, with permission, from Winkelmann et al.[85] Copyright 2009, Springer Nature.

(C) Energy levels of the YSR bound states measured on MnPc/Pb(111) exhibit continuous evolution, accompanied by the emergence of Kondo resonant peaks. Reprinted, with permission, from Franke et al.[86] Copyright 2011, American Association for the Advancement of Science.

(D) Scanning tunneling spectroscopy spectra revealing the modulation of molecular YSR states by MnPc molecular moiré patterns, leading to quantum phase transitions. Reprinted, with permission, from Hatter et al.[87] Copyright 2015, Springer Nature.

(E) Spatial distribution of the YSR states investigated by varying the tunneling current to adjust the tip-sample distance within the Tb_2Pc_3 molecule. Reprinted, with permission, from Xia et al.[88] Copyright 2022, Springer Nature.

(F) Distance-dependent d*I*/d*V* spectra, elucidating the long-lived excited spin states of Fe-octaethylporphyrin-chloride/Pb(111). The intensities of both inelastic excitations increase, and the excitation energy shifts to higher values as the distance decreases. Reprinted, with permission, from Heinrich et al.[89] Copyright 2013, Springer Nature.

(G) Schematic representation of single-atom Josephson junctions comprising Pb, Mn, and Cr atoms. The inset presents an STM topography of a Pb(111) surface, highlighting individual Pb, Mn, and Cr adatoms with colored circles. Reprinted, with permission, from Trahms et al.[90] Copyright 2023, Springer Nature.

interplay between spin and superconductivity provide a rich experimental basis for studying quantum phenomena at the nanoscale.

Conclusion and outlook

Molecular-scale spintronics, as pioneering quantum technology, transforms our understanding of microscopic physical

phenomena and creates new avenues in sensing, data storage, and quantum computing.[95–97] This review elucidates three key interactions of spin effects at the molecular scale. To commence, exchange coupling and the Kondo effect are critical phenomena that substantially influence the molecular spin states and electronic transport characteristics. Moreover, the interaction between spin and electric/magnetic fields is crucial for precise spin control and quantum information processing. The MR effect focuses on the interplay among magnetic fields, molecular structure, and spin-polarized transport, offering new insights for the design and development of next-generation memory devices. In addition, CISS empowers non-magnetic chiral molecules to achieve selective spin filtering due to their unique structural features, even in the absence of an external magnetic field. Among the most compelling frontier topics in spintronics is the interplay between spin phenomena and superconductivity at the nanoscale. An in-depth understanding of the interactions between Cooper pairs in single-molecule superconducting systems and conducting molecules unveils the competitive relationship between superconductivity and the Kondo effect. Moreover, studies on atomic-scale YSR states expand the application potential of superconducting electronic devices.

Looking ahead, several key research directions can broaden the foundational physical phenomena and applications of molecular-scale spintronics. First, integrating a molecular spin center into a device architecture may alter its electronic structure and magnetic properties, leading to the loss of quantum coherence. A critical challenge lies in achieving effective molecular connections while preserving intrinsic molecular magnetism, where graphene-based device architectures may open new possibilities.[25,98] Second, achieving stable and controllable spin behavior at room temperature is another critical goal. Progress in SMMs suggests promising potential for room-temperature spin manipulation.[13,49] Third, the rise of nuclear electric resonance techniques has brought new opportunities to this field,[99] enabling more precise detection and control of nuclear spins. However, nuclear spin control remains an emerging area, requiring continued exploration of diverse spin-related phenomena. Fourth, enhancing the integration of single-molecule detection with complementary techniques to probe individual spin states is crucial. For instance, the ESR-atomic force microscopy/STM technology enables both the detection and manipulation of electron spin-state transitions.[21,22] Future investigations into spin phenomena within superconducting systems, particularly in the context of quantum bit technology, merit heightened attention and dedicated exploration. The intrinsic properties of individual molecules may induce unconventional effects within superconducting Josephson junctions, offering significant potential for qubit manipulation and readout. Finally, the recent advancements in artificial intelligence hold promising potential for enhancing single-molecule detection.[100] In particular, the application of machine learning in capturing subtle spin signals and mining complex data is expected to deepen physical insights and extend device functionalities.

In summary, molecular-scale spintronics is steadily emerging as a pivotal field in information technology, materials science, and quantum science. Its progress promises to drive a new era of information technology, with novel spintronic devices that offer higher storage densities and processing speeds alongside breakthroughs in quantum computing technology.

ACKNOWLEDGMENTS

The authors acknowledge primary financial support from the National Key R&D Program of China (2021YFA1200101, 2022YFE0128700, and 2023YFF1205803), the National Natural Science Foundation of China (22150013 and 21933001), Beijing National Laboratory for Molecular Sciences (BNLMS-CXXM-202407), and "Frontiers Science Center for New Organic Matter" at Nankai University (63181206).

AUTHOR CONTRIBUTIONS

X.G. proposed the topic and supervised the review. C.Y., H.W., and J.C. investigated the literature and wrote the draft manuscript. X.G. reviewed and revised the manuscript.

DECLARATION OF INTERESTS

X.G. is a member of *Newton*'s advisory board.

REFERENCES

1. Zutic, I., Fabian, J., and Das Sarma, S. (2004). Spintronics: fundamentals and applications. Rev. Mod. Phys. *76*, 323–410. https://doi.org/10.1103/RevModPhys.76.323.
2. Baibich, M.N., Broto, J.M., Fert, A., Nguyen Van Dau, F., Petroff, F., Etienne, P., Creuzet, G., Friederich, A., and Chazelas, J. (1988). Magnetoresistance of (001)Fe/(001)Cr magnetic superlattices. Phys. Rev. Lett. *61*, 2472–2475. https://doi.org/10.1103/PhysRevLett.61.2472.
3. Ferrando-Soria, J., Vallejo, J., Castellano, M., Martínez-Lillo, J., Pardo, E., Cano, J., Castro, I., Lloret, F., Ruiz-García, R., and Julve, M. (2017). Molecular magnetism, quo vadis? A historical perspective from a coordination chemist viewpoint. Coord. Chem. Rev. *339*, 17–103. https://doi.org/10.1016/j.ccr.2017.03.004.
4. Forment-Aliaga, A., and Gaita-Arino, A. (2022). Chiral, magnetic, molecule-based materials: A chemical path toward spintronics and quantum nanodevices. J. Appl. Phys. *132*, 180901. https://doi.org/10.1063/5.0118582.
5. Maylander, M., Thielert, P., Quintes, T., Vargas Jentzsch, A., and Richert, S. (2023). Room temperature electron spin coherence in photogenerated molecular spin qubit candidates. J. Am. Chem. Soc. *145*, 14064–14069. https://doi.org/10.1021/jacs.3c04021.
6. Li, L., Prindle, C.R., Shi, W., Nuckolls, C., and Venkataraman, L. (2023). Radical single-molecule junctions. J. Am. Chem. Soc. *145*, 18182–18204. https://doi.org/10.1021/jacs.3c04487.
7. Zakrzewski, J.J., Liberka, M., Wang, J., Chorazy, S., and Ohkoshi, S.I. (2024). Optical phenomena in molecule-based magnetic materials. Chem. Rev. *124*, 5930–6050. https://doi.org/10.1021/acs.chemrev.3c00840.
8. Kumar, K.S., and Ruben, M. (2021). Sublimable spin-crossover complexes: From spin-state switching to molecular devices. Angew. Chem. Int. Ed. *60*, 7502–7521. https://doi.org/10.1002/anie.201911256.
9. Xu, Z., Liu, J., Hou, S., and Wang, Y. (2020). Manipulation of molecular spin state on surfaces studied by scanning tunneling microscopy. Nanomaterials *10*, 2393. https://doi.org/10.3390/nano10122393.
10. Shang, Z., Liu, T., Yang, Q., Cui, S., Xu, K., Zhang, Y., Deng, J., Zhai, T., and Wang, X. (2022). Chiral-molecule-based spintronic devices. Small *18*, 2203015. https://doi.org/10.1002/smll.202203015.

11. Naaman, R., Paltiel, Y., and Waldeck, D.H. (2019). Chiral molecules and the electron spin. Nat. Rev. Chem *3*, 250–260. https://doi.org/10.1038/s41570-019-0087-1.

12. Coronado, E. (2019). Molecular magnetism: From chemical design to spin control in molecules, materials and devices. Nat. Rev. Mater. *5*, 87–104. https://doi.org/10.1038/s41578-019-0146-8.

13. Moreno-Pineda, E., and Wernsdorfer, W. (2021). Measuring molecular magnets for quantum technologies. Nat. Rev. Phys. *3*, 645–659. https://doi.org/10.1038/s42254-021-00340-3.

14. Blagg, R.J., Ungur, L., Tuna, F., Speak, J., Comar, P., Collison, D., Wernsdorfer, W., McInnes, E.J.L., Chibotaru, L.F., and Winpenny, R.E. P. (2013). Magnetic relaxation pathways in lanthanide single-molecule magnets. Nat. Chem. *5*, 673–678. https://doi.org/10.1038/nchem.1707.

15. Bloom, B.P., Paltiel, Y., Naaman, R., and Waldeck, D.H. (2024). Chiral induced spin selectivity. Chem. Rev. *124*, 1950–1991. https://doi.org/10.1021/acs.chemrev.3c00661.

16. Bloom, B.P., Chen, Z., Lu, H., and Waldeck, D.H. (2024). A chemical perspective on the chiral induced spin selectivity effect. Natl. Sci. Rev. *11*, nwae212. https://doi.org/10.1093/nsr/nwae212.

17. Loth, S., Baumann, S., Lutz, C.P., Eigler, D.M., and Heinrich, A.J. (2012). Bistability in atomic-scale antiferromagnets. Science *335*, 196–199. https://doi.org/10.1126/science.1214131.

18. de Bruijckere, J., Gehring, P., Palacios-Corella, M., Clemente-León, M., Coronado, E., Paaske, J., Hedegård, P., and van der Zant, H.S.J. (2019). Ground-state spin blockade in a single-molecule junction. Phys. Rev. Lett. *122*, 197701. https://doi.org/10.1103/PhysRevLett.122.197701.

19. Liang, W., Shores, M.P., Bockrath, M., Long, J.R., and Park, H. (2002). Kondo resonance in a single-molecule transistor. Nature *417*, 725–729. https://doi.org/10.1038/nature00790.

20. Park, J., Pasupathy, A.,N., Goldsmith, J.I., Chang, C., Yaish, Y., Petta, J. R., Rinkoski, M., Sethna, J.P., Abruña, H.D., McEuen, P.L., and Ralph, D. C. (2002). Coulomb blockade and the Kondo effect in single-atom transistors. Nature *417*, 722–725. https://doi.org/10.1038/nature00791.

21. Sellies, L., Spachtholz, R., Bleher, S., Eckrich, J., Scheuerer, P., and Repp, J. (2023). Single-molecule electron spin resonance by means of atomic force microscopy. Nature *624*, 64–68. https://doi.org/10.1038/s41586-023-06754-6.

22. Kovarik, S., Schlitz, R., Vishwakarma, A., Ruckert, D., Gambardella, P., and Stepanow, S. (2024). Spin torque–driven electron paramagnetic resonance of a single spin in a pentacene molecule. Science *384*, 1368–1373. https://doi.org/10.1126/science.adh4753.

23. Willke, P., Bilgeri, T., Zhang, X., Wang, Y., Wolf, C., Aubin, H., Heinrich, A., and Choi, T. (2021). Coherent spin control of single molecules on a surface. ACS Nano *15*, 17959–17965. https://doi.org/10.1021/acsnano.1c06394.

24. Slota, M., and Bogani, L. (2020). Combining molecular spintronics with electron paramagnetic resonance: the path towards single-molecule pulsed spin spectroscopy. Appl. Magn. Reson. *51*, 1357–1409. https://doi.org/10.1007/s00723-020-01292-0.

25. Pei, T., Thomas, J.O., Sopp, S., Tsang, M.-Y., Dotti, N., Baugh, J., Chilton, N.F., Cardona-Serra, S., Gaita-Ariño, A., Anderson, H.L., and Bogani, L. (2022). Exchange-induced spin polarization in a single magnetic molecule junction. Nat. Commun. *13*, 4506. https://doi.org/10.1038/s41467-022-31909-w.

26. Oberg, J.C., Calvo, M.R., Delgado, F., Moro-Lagares, M., Serrate, D., Jacob, D., Fernández-Rossier, J., and Hirjibehedin, C.F. (2014). Control of single-spin magnetic anisotropy by exchange coupling. Nat. Nanotechnol. *9*, 64–68. https://doi.org/10.1038/nnano.2013.264.

27. Campbell, V.E., Tonelli, M., Cimatti, I., Moussy, J.-B., Tortech, L., Dappe, Y.J., Rivière, E., Guillot, R., Delprat, S., Mattana, R., et al. (2016). Engineering the magnetic coupling and anisotropy at the molecule–magnetic surface interface in molecular spintronic devices. Nat. Commun. *7*, 13646. https://doi.org/10.1038/ncomms13646.

28. Yan, S., Choi, D.-J., Burgess, J.A.J., Rolf-Pissarczyk, S., and Loth, S. (2015). Control of quantum magnets by atomic exchange bias. Nat. Nanotechnol. *10*, 40–45. https://doi.org/10.1038/nnano.2014.281.

29. Gaudenzi, R., de Bruijckere, J., Reta, D., Moreira, I.d.P.R., Rovira, C., Veciana, J., van der Zant, H.S.J., and Burzurí, E. (2017). Redox-induced gating of the exchange interactions in a single organic diradical. ACS Nano *11*, 5879–5883. https://doi.org/10.1021/acsnano.7b01578.

30. de Haas, W.J., de Boer, J., and van dën Berg, G.J. (1934). The electrical resistance of gold, copper and lead at low temperatures. Physica *1*, 1115–1124. https://doi.org/10.1016/S0031-8914(34)80310-2.

31. Sarachik, M.P., Corenzwit, E., and Longinotti, L.D. (1964). Resistivity of Mo-Nb and Mo-Re alloys containing 1% Fe. Phys. Rev. *135*, A1041–A1045. https://doi.org/10.1103/PhysRev.135.A1041.

32. Kondo, J. (1964). Resistance minimum in dilute magnetic alloys. Prog. Theor. Phys. *32*, 37–49. https://doi.org/10.1143/PTP.32.37.

33. Gehring, P., Thijssen, J.M., and van der Zant, H.S.J. (2019). Single-molecule quantum-transport phenomena in break junctions. Nat. Rev. Phys. *1*, 381–396. https://doi.org/10.1038/s42254-019-0055-1.

34. Scott, G.D., and Natelson, D. (2010). Kondo resonances in molecular devices. ACS Nano *4*, 3560–3579. https://doi.org/10.1021/nn100793s.

35. Parks, J.J., Champagne, A.R., Costi, T.A., Shum, W.W., Pasupathy, A.N., Neuscamman, E., Flores-Torres, S., Cornaglia, P.S., Aligia, A.A., Balseiro, C.A., et al. (2010). Mechanical control of spin states in spin-1 molecules and the underscreened Kondo effect. Science *328*, 1370–1373. https://doi.org/10.1126/science.1186874.

36. Köbke, A., Gutzeit, F., Röhricht, F., Schlimm, A., Grunwald, J., Tuczek, F., Studniarek, M., Longo, D., Choueikani, F., Otero, E., et al. (2020). Reversible coordination-induced spin-state switching in complexes on metal surfaces. Nat. Nanotechnol. *15*, 18–21. https://doi.org/10.1038/s41565-019-0594-8.

37. Frisenda, R., Gaudenzi, R., Franco, C., Mas-Torrent, M., Rovira, C., Veciana, J., Alcon, I., Bromley, S.T., Burzurí, E., and van der Zant, H.S.J. (2015). Kondo effect in a neutral and stable all organic radical single molecule break junction. Nano Lett. *15*, 3109–3114. https://doi.org/10.1021/acs.nanolett.5b00155.

38. Guo, X., Zhu, Q., Zhou, L., Yu, W., Lu, W., and Liang, W. (2021). Evolution and universality of two-stage Kondo effect in single manganese phthalocyanine molecule transistors. Nat. Commun. *12*, 1566. https://doi.org/10.1038/s41467-021-21492-x.

39. Yu, L.H., and Natelson, D. (2004). The Kondo effect in C60 single-molecule transistors. Nano Lett. *4*, 79–83. https://doi.org/10.1021/nl034893f.

40. Zhao, A., Li, Q., Chen, L., Xiang, H., Wang, W., Pan, S., Wang, B., Xiao, X., Yang, J., Hou, J.G., and Zhu, Q. (2005). Controlling the kondo effect of an adsorbed magnetic ion through its chemical bonding. Science *309*, 1542–1544. https://doi.org/10.1126/science.1113449.

41. Calvo, M.R., Fernández-Rossier, J., Palacios, J.J., Jacob, D., Natelson, D., and Untiedt, C. (2009). The Kondo effect in ferromagnetic atomic contacts. Nature *458*, 1150–1153. https://doi.org/10.1038/nature07878.

42. Miyamachi, T., Gruber, M., Davesne, V., Bowen, M., Boukari, S., Joly, L., Scheurer, F., Rogez, G., Yamada, T.K., Ohresser, P., et al. (2012). Robust spin crossover and memristance across a single molecule. Nat. Commun. *3*, 938. https://doi.org/10.1038/ncomms1940.

43. Wagner, S., Kisslinger, F., Ballmann, S., Schramm, F., Chandrasekar, R., Bodenstein, T., Fuhr, O., Secker, D., Fink, K., Ruben, M., and Weber, H.B. (2013). Switching of a coupled spin pair in a single-molecule junction. Nat. Nanotechnol. *8*, 575–579. https://doi.org/10.1038/nnano.2013.133.

44. Harzmann, G.D., Frisenda, R., van der Zant, H.S.J., and Mayor, M. (2015). Single-molecule spin switch based on voltage-triggered distortion of the coordination sphere. Angew. Chem. Int. Ed. *54*, 13425–13430. https://doi.org/10.1002/anie.201505447.

45. Li, P., Zhou, L., Zhao, C., Ju, H., Gao, Q., Si, W., Cheng, L., Hao, J., Li, M., Chen, Y., et al. (2022). Single-molecule nano-optoelectronics: insights

from physics. Rep. Prog. Phys. *85*, 086401. https://doi.org/10.1088/1361-6633/ac7401.

46. Meded, V., Bagrets, A., Fink, K., Chandrasekar, R., Ruben, M., Evers, F., Bernand-Mantel, A., Seldenthuis, J.S., Beukman, A., and van der Zant, H. S.J. (2011). Electrical control over the Fe(II) spin crossover in a single molecule: Theory and experiment. Phys. Rev. B *83*, 245415. https://doi.org/10.1103/PhysRevB.83.245415.
47. Vincent, R., Klyatskaya, S., Ruben, M., Wernsdorfer, W., and Balestro, F. (2012). Electronic read-out of a single nuclear spin using a molecular spin transistor. Nature *488*, 357–360. https://doi.org/10.1038/nature11341.
48. Urdampilleta, M., Klayatskaya, S., Ruben, M., and Wernsdorfer, W. (2015). Magnetic interaction between a radical spin and a single-molecule magnet in a molecular spin-valve. ACS Nano *9*, 4458–4464. https://doi.org/10.1021/acsnano.5b01056.
49. Thiele, S., Balestro, F., Ballou, R., Klyatskaya, S., Ruben, M., and Wernsdorfer, W. (2014). Electrically driven nuclear spin resonance in single-molecule magnets. Science *344*, 1135–1138. https://doi.org/10.1126/science.1249802.
50. Pyurbeeva, E., Hsu, C., Vogel, D., Wegeberg, C., Mayor, M., van der Zant, H., Mol, J.A., and Gehring, P. (2021). Controlling the entropy of a single-molecule junction. Nano Lett. *21*, 9715–9719. https://doi.org/10.1021/acs.nanolett.1c03591.
51. Yang, C., Chen, Z., Yu, C., Cao, J., Ke, G., Zhu, W., Liang, W., Huang, J., Cai, W., Saha, C., et al. (2024). Regulation of quantum spin conversions in a single molecular radical. Nat. Nanotechnol. *19*, 978–985. https://doi.org/10.1038/s41565-024-01632-2.
52. Pyurbeeva, E., Mol, J.A., and Gehring, P. (2022). Electronic measurements of entropy in meso- and nanoscale systems. Chem. Phys. Rev. *3*, 041308. https://doi.org/10.1063/5.0101784.
53. Pyurbeeva, E., and Mol, J.A. (2021). A thermodynamic approach to measuring entropy in a few-electron nanodevice. Entropy *23*, 640. https://doi.org/10.3390/e23060640.
54. Guo, L., Gu, X., Zhu, X., and Sun, X. (2019). Recent advances in molecular spintronics: Multifunctional spintronic devices. Adv. Mater. *31*, 1805355. https://doi.org/10.1002/adma.201805355.
55. Natterer, F.D., Yang, K., Paul, W., Willke, P., Choi, T., Greber, T., Heinrich, A.J., and Lutz, C.P. (2017). Reading and writing single-atom magnets. Nature *543*, 226–228. https://doi.org/10.1038/nature21371.
56. Barraud, C., Seneor, P., Mattana, R., Fusil, S., Bouzehouane, K., Deranlot, C., Graziosi, P., Hueso, L., Bergenti, I., Dediu, V., et al. (2010). Unravelling the role of the interface for spin injection into organic semiconductors. Nat. Phys. *6*, 615–620. https://doi.org/10.1038/nphys1688.
57. Sanvito, S. (2010). The rise of spinterface science. Nat. Phys. *6*, 562–564. https://doi.org/10.1038/nphys1714.
58. Wang, F., Shen, W., Shui, Y., Chen, J., Wang, H., Wang, R., Qin, Y., Wang, X., Wan, J., Zhang, M., et al. (2024). Electrically controlled nonvolatile switching of single-atom magnetism in a Dy@C84 single-molecule transistor. Nat. Commun. *15*, 2450. https://doi.org/10.1038/s41467-024-46854-z.
59. Hayakawa, R., Karimi, M.A., Wolf, J., Huhn, T., Zöllner, M.S., Herrmann, C., and Scheer, E. (2016). Large magnetoresistance in single-radical molecular junctions. Nano Lett. *16*, 4960–4967. https://doi.org/10.1021/acs.nanolett.6b01595.
60. Yang, K., Chen, H., Pope, T., Hu, Y., Liu, L., Wang, D., Tao, L., Xiao, W., Fei, X., Zhang, Y.-Y., et al. (2019). Tunable giant magnetoresistance in a single-molecule junction. Nat. Commun. *10*, 3599. https://doi.org/10.1038/s41467-019-11587-x.
61. Schmaus, S., Bagrets, A., Nahas, Y., Yamada, T.K., Bork, A., Bowen, M., Beaurepaire, E., Evers, F., and Wulfhekel, W. (2011). Giant magnetoresistance through a single molecule. Nat. Nanotechnol. *6*, 185–189. https://doi.org/10.1038/nnano.2011.11.
62. Li, J.-J., Bai, M.-L., Chen, Z.-B., Zhou, X.-S., Shi, Z., Zhang, M., Ding, S.-Y., Hou, S.-M., Schwarzacher, W., Nichols, R.J., and Mao, B.W. (2015). Giant single-molecule anisotropic magnetoresistance at room temperature. J. Am. Chem. Soc. *137*, 5923–5929. https://doi.org/10.1021/ja512483y.
63. Cinchetti, M., Dediu, V.A., and Hueso, L.E. (2017). Activating the molecular spinterface. Nat. Mater. *16*, 507–515. https://doi.org/10.1038/nmat4902.
64. Zhan, Y., Holmström, E., Lizárraga, R., Eriksson, O., Liu, X., Li, F., Carlegrim, E., Stafström, S., and Fahlman, M. (2010). Efficient spin injection through exchange coupling at organic semiconductor/ferromagnet heterojunctions. Adv. Mater. *22*, 1626–1630. https://doi.org/10.1002/adma.200903556.
65. Steil, S., Großmann, N., Laux, M., Ruffing, A., Steil, D., Wiesenmayer, M., Mathias, S., Monti, O.L.A., Cinchetti, M., and Aeschlimann, M. (2013). Spin-dependent trapping of electrons at spinterfaces. Nat. Phys. *9*, 242–247. https://doi.org/10.1038/nphys2548.
66. Ray, K., Ananthavel, S.P., Waldeck, D.H., and Naaman, R. (1999). Asymmetric scattering of polarized electrons by organized organic films of chiral molecules. Science *283*, 814–816. https://doi.org/10.1126/science.283.5403.814.
67. Xie, Z., Markus, T.Z., Cohen, S.R., Vager, Z., Gutierrez, R., and Naaman, R. (2011). Spin specific electron conduction through DNA oligomers. Nano Lett. *11*, 4652–4655. https://doi.org/10.1021/nl2021637.
68. Göhler, B., Hamelbeck, V., Markus, T.Z., Kettner, M., Hanne, G.F., Vager, Z., Naaman, R., and Zacharias, H. (2011). Spin selectivity in electron transmission through self-assembled monolayers of double-stranded DNA. Science *331*, 894–897. https://doi.org/10.1126/science.1199339.
69. Torres-Cavanillas, R., Escorcia-Ariza, G., Brotons-Alcázar, I., Sanchis-Gual, R., Mondal, P.C., Rosaleny, L.E., Giménez-Santamarina, S., Sessolo, M., Galbiati, M., Tatay, S., et al. (2020). Reinforced room-temperature spin filtering in chiral paramagnetic metallopeptides. J. Am. Chem. Soc. *142*, 17572–17580. https://doi.org/10.1021/jacs.0c07531.
70. Banerjee-Ghosh, K., Ben Dor, O., Tassinari, F., Capua, E., Yochelis, S., Capua, A., Yang, S.-H., Parkin, S.S.P., Sarkar, S., Kronik, L., et al. (2018). Separation of enantiomers by their enantiospecific interaction with achiral magnetic substrates. Science *360*, 1331–1334. https://doi.org/10.1126/science.aar4265.
71. Safari, M.R., Matthes, F., Schneider, C.M., Ernst, K.-H., and Bürgler, D.E. (2024). Spin-selective electron transport through single chiral molecules. Small *20*, 2308233. https://doi.org/10.1002/smll.202308233.
72. Kiran, V., Mathew, S.P., Cohen, S.R., Hernández Delgado, I., Lacour, J., and Naaman, R. (2016). Helicenes-a new class of organic spin filter. Adv. Mater. *28*, 1957–1962. https://doi.org/10.1002/adma.201504725.
73. Qian, Q., Ren, H., Zhou, J., Wan, Z., Zhou, J., Yan, X., Cai, J., Wang, P., Li, B., Sofer, Z., et al. (2022). Chiral molecular intercalation superlattices. Nature *606*, 902–908. https://doi.org/10.1038/s41586-022-04846-3.
74. Kim, Y.-H., Zhai, Y., Lu, H., Pan, X., Xiao, C., Gaulding, E.A., Harvey, S.P., Berry, J.J., Vardeny, Z.V., Luther, J.M., and Beard, M.C. (2021). Chiral-induced spin selectivity enables a room-temperature spin light-emitting diode. Science *371*, 1129–1133. https://doi.org/10.1126/science.abf5291.
75. Yang, C., Li, Y., Zhou, S., Guo, Y., Jia, C., Liu, Z., Houk, K.N., Dubi, Y., and Guo, X. (2023). Real-time monitoring of reaction stereochemistry through single-molecule observations of chirality-induced spin selectivity. Nat. Chem. *15*, 972–979. https://doi.org/10.1038/s41557-023-01212-2.
76. Evers, F., Aharony, A., Bar-Gill, N., Entin-Wohlman, O., Hedegård, P., Hod, O., Jelinek, P., Kamieniarz, G., Lemeshko, M., Michaeli, K., et al. (2022). Theory of chirality induced spin selectivity: progress and challenges. Adv. Mater. *34*, 2106629. https://doi.org/10.1002/adma.202106629.

77. Das, T.K., Tassinari, F., Naaman, R., and Fransson, J. (2022). Temperature-dependent chiral-induced spin selectivity effect: experiments and theory. J. Phys. Chem. C *126*, 3257–3264. https://doi.org/10.1021/acs.jpcc.1c10550.

78. Ohe, K., Shishido, H., Kato, M., Utsumi, S., Matsuura, H., and Togawa, Y. (2024). Chirality-induced selectivity of phonon angular momenta in chiral quartz crystals. Phys. Rev. Lett. *132*, 056302. https://doi.org/10.1103/PhysRevLett.132.056302.

79. Liu, Y., Xiao, J., Koo, J., and Yan, B. (2021). Chirality-driven topological electronic structure of DNA-like materials. Nat. Mater. *20*, 638–644. https://doi.org/10.1038/s41563-021-00924-5.

80. Adhikari, Y., Liu, T., Wang, H., Hua, Z., Liu, H., Lochner, E., Schlottmann, P., Yan, B., Zhao, J., and Xiong, P. (2023). Interplay of structural chirality, electron spin and topological orbital in chiral molecular spin valves. Nat. Commun. *14*, 5163. https://doi.org/10.1038/s41467-023-40884-9.

81. Heinrich, B.W., Pascual, J.I., and Franke, K.J. (2018). Single magnetic adsorbates on s -wave superconductors. Prog. Surf. Sci. *93*, 1–19. https://doi.org/10.1016/j.progsurf.2018.01.001.

82. Yu, L. (1965). Bound state in superconducors with paramagnetic impurities. Acta Phys. Sin. *21*, 75–91.

83. Shiba, H. (1968). Classical spins in superconductors. Prog. Theor. Phys. *40*, 435–451. https://doi.org/10.1143/PTP.40.435.

84. Rusinov, A.I. (1969). On the theory of gapless superconductivity in alloys containing paramagnetic impurities. Sov. Phys. JETP *29*, 1101–1106.

85. Winkelmann, C.B., Roch, N., Wernsdorfer, W., Bouchiat, V., and Balestro, F. (2009). Superconductivity in a single-C60 transistor. Nat. Phys. *5*, 876–879. https://doi.org/10.1038/nphys1433.

86. Franke, K.J., Schulze, G., and Pascual, J.I. (2011). Competition of superconducting phenomena and Kondo screening at the nanoscale. Science *332*, 940–944. https://doi.org/10.1126/science.1202204.

87. Hatter, N., Heinrich, B.W., Ruby, M., Pascual, J.I., and Franke, K.J. (2015). Magnetic anisotropy in Shiba bound states across a quantum phase transition. Nat. Commun. *6*, 8988. https://doi.org/10.1038/ncomms9988.

88. Xia, H.-N., Minamitani, E., Žitko, R., Liu, Z.-Y., Liao, X., Cai, M., Ling, Z.-H., Zhang, W.-H., Klyatskaya, S., Ruben, M., and Fu, Y.S. (2022). Spin-orbital Yu-Shiba-Rusinov states in single Kondo molecular magnet. Nat. Commun. *13*, 6388. https://doi.org/10.1038/s41467-022-34187-8.

89. Heinrich, B.W., Braun, L., Pascual, J.I., and Franke, K.J. (2013). Protection of excited spin states by a superconducting energy gap. Nat. Phys. *9*, 765–768. https://doi.org/10.1038/nphys2794.

90. Trahms, M., Melischek, L., Steiner, J.F., Mahendru, B., Tamir, I., Bogdanoff, N., Peters, O., Reecht, G., Winkelmann, C.B., von Oppen, F., and Franke, K.J. (2023). Diode effect in Josephson junctions with a single magnetic atom. Nature *615*, 628–633. https://doi.org/10.1038/s41586-023-05743-z.

91. Katzir, E., Sukenik, N., Kalcheim, Y., Alpern, H., Yochelis, S., Berlin, Y.A., Ratner, M.A., Millo, O., and Paltiel, Y. (2017). Probing molecular-transport properties using the superconducting proximity effect. Small Methods *1*, 1600034. https://doi.org/10.1002/smtd.201600034.

92. Küster, F., Montero, A.M., Guimarães, F.S.M., Brinker, S., Lounis, S., Parkin, S.S.P., and Sessi, P. (2021). Correlating Josephson supercurrents and Shiba states in quantum spins unconventionally coupled to superconductors. Nat. Commun. *12*, 1108. https://doi.org/10.1038/s41467-021-21347-5.

93. Periyasamy, M., Bradshaw, H., Sukenik, N., Alpern, H., Yochelis, S., Robinson, J.W.A., Millo, O., and Paltiel, Y. (2020). Universal proximity effects in hybrid superconductor-linker molecule-nanoparticle systems: The effect of molecular chirality. Appl. Phys. Lett. *117*, 242601. https://doi.org/10.1063/5.0030892.

94. Xing, Y., Chen, H., Hu, B., Ye, Y., Hofer, W.A., and Gao, H.-J. (2022). Reversible switching of Kondo resonance in a single-molecule junction. Nano Res. *15*, 1466–1471. https://doi.org/10.1007/s12274-021-3688-1.

95. Fétida, A., Bengone, O., Romeo, M., Scheurer, F., Robles, R., Lorente, N., and Limot, L. (2024). Single-spin sensing: A molecule-on-tip approach. ACS Nano *18*, 13829–13835. https://doi.org/10.1021/acsnano.4c02470.

96. Heinrich, A.J., Oliver, W.D., Vandersypen, L.M.K., Ardavan, A., Sessoli, R., Loss, D., Jayich, A.B., Fernandez-Rossier, J., Laucht, A., and Morello, A. (2021). Quantum-coherent nanoscience. Nat. Nanotechnol. *16*, 1318–1329. https://doi.org/10.1038/s41565-021-00994-1.

97. Gaita-Arino, A., Luis, F., Hill, S., and Coronado, E. (2019). Molecular spins for quantum computation. Nat. Chem. *11*, 301–309. https://doi.org/10.1038/s41557-019-0232-y.

98. Candini, A., Klyatskaya, S., Ruben, M., Wernsdorfer, W., and Affronte, M. (2011). Graphene spintronic devices with molecular nanomagnets. Nano Lett. *11*, 2634–2639. https://doi.org/10.1021/nl2006142.

99. Asaad, S., Mourik, V., Joecker, B., Johnson, M.A.I., Baczewski, A.D., Firgau, H.R., Mądzik, M.T., Schmitt, V., Pla, J.J., Hudson, F.E., et al. (2020). Coherent electrical control of a single high-spin nucleus in silicon. Nature *579*, 205–209. https://doi.org/10.1038/s41586-020-2057-7.

100. Yan, C., Fang, C., Gan, J., Wang, J., Zhao, X., Wang, X., Li, J., Zhang, Y., Liu, H., Li, X., et al. (2024). From molecular electronics to molecular intelligence. ACS Nano *18*, 28531–28556. https://doi.org/10.1021/acsnano.4c10389.